

# Deconstructed Higgsless Models with One-Site Delocalization

---

**R. Sekhar Chivukula and Elizabeth H. Simmons**

*Department of Physics and Astronomy, Michigan State University*

*East Lansing, MI 48824, USA*

*E-mail: sekhar@msu.edu, esimmons@msu.edu*

**Hong-Jian He**

*Department of Physics, University of Texas*

*Austin, TX 78712, USA*

*E-mail: hjhe@physics.utexas.edu*

**Masafumi Kurachi**

*Department of Physics, Nagoya University*

*Nagoya 464-8602, Japan*

*E-mail: kurachi@eken.phys.nagoya-u.ac.jp*

**Masaharu Tanabashi**

*Department of Physics, Tohoku University*

*Sendai 980-8578, Japan*

*E-mail: tanabash@tuhep.phys.tohoku.ac.jp*

**ABSTRACT:** In this note we calculate the form of electroweak corrections in deconstructed Higgsless models for the case of a fermion whose weak properties arise from two adjacent  $SU(2)$  groups on the deconstructed lattice. We show that, as recently proposed in the continuum, it is possible for the value of the electroweak parameter  $\alpha S$  to be small in such a model. In addition, by working in the deconstructed limit, we may directly evaluate the size of off- $Z$ -pole electroweak corrections arising from the exchange of Kaluza-Klein modes; this has not been studied in the continuum. The size of these corrections is summarized by the electroweak parameter  $\alpha\delta$ . In one-site delocalized Higgsless models with small values of  $\alpha S$ , we show that the amount of delocalization is bounded from above, and must be less than 25% at 95% CL. We discuss the relation of these calculations to our previous calculations in deconstructed Higgsless models, and to models of extended technicolor. We present numerical results for a four-site model, illustrating our analytic calculations.

KEYWORDS: Dimensional Deconstruction, Electroweak Symmetry Breaking, Higgsless Theories, Delocalization.

## 1. Introduction

“Higgsless” models [1] have emerged as an intriguing direction for research into the origin of electroweak symmetry breaking. In these models, which are based on five-dimensional gauge theories compactified on an interval, unitarization of the electroweak bosons’ self-interactions occurs through the exchange of a tower of massive vector bosons [2, 3, 4, 5], rather than the exchange of a scalar Higgs boson [6].

We have recently analyzed the electroweak corrections in a large class of Higgsless models in which the fermions are localized within the extra dimension [7, 8, 9]. Specifically, we studied all Higgsless models which can be deconstructed [10, 11] to a chain of  $SU(2)$  gauge groups adjacent to a chain of  $U(1)$  gauge groups, with the fermions coupled to any single  $SU(2)$  group and to any single  $U(1)$  group along the chain. Our use of deconstruction allowed us to relate the size of corrections to electroweak processes directly to the spectrum of vector bosons (“Kaluza-Klein modes”) which, in Higgsless models, is constrained by unitarity. Our results apply for arbitrary background 5-D geometry, spatially dependent gauge-couplings, and brane kinetic energy terms.

We found [7] that Higgsless models with localized fermions which do not have extra light vector bosons (with masses of order the  $W$  and  $Z$  masses) cannot simultaneously satisfy the constraints of precision electroweak data and unitarity bounds. In particular, we found that unitarity constrains the electroweak parameter  $\hat{S}$  as follows

$$\hat{S} = \frac{1}{4s^2} \left( \alpha S + 4c^2(\Delta\rho - \alpha T) + \frac{\alpha\delta}{c^2} \right) \geq M_W^2 \Sigma_r \geq \frac{M_W^2}{8\pi v^2} \simeq 4 \times 10^{-3} . \quad (1.1)$$

This large a value is disfavored by precision electroweak data [12].

Although we framed those results in terms of their application to continuum Higgsless 5-D models, they also apply far from the continuum limit when only a few extra vector bosons are present. As such, these results form a generalization of phenomenological analyses [13] of models of extended electroweak gauge symmetries [14, 15, 16] motivated by models of hidden local symmetry [17, 18, 19, 20, 21]. Our previous results are complementary to, and more general than, the analyses of the phenomenology of these models in the continuum [22, 23, 24, 25, 26, 27, 28, 12, 29]. They also apply independent of the form of the high-energy completion of the Higgsless theory; the potentially large higher-order corrections expected to be present in QCD-like completions have been discussed in [30].

It has been proposed [31, 32] that the size of corrections to electroweak processes may be reduced by allowing for delocalized fermions. We now investigate this possibility in the context of deconstruction. This paper will focus on the effects of adding fermion delocalization to the deconstructed models which our earlier work identified as having the greatest phenomenological promise (i.e., those in which the electroweak corrections are smallest). These are models (designated “Case I”) in which the fermions’ hypercharge interactions are with the  $U(1)$  group at the interface between the  $SU(2)$  and  $U(1)$  groups, and in which the gauge couplings of that  $U(1)$  group and of the  $SU(2)$  group farthest from the interface are small.

For simplicity, we will assume, in this paper, that the  $U(1)$  group adjacent to the interface is the only hypercharge group in the model; this corresponds to taking the  $M = 0$  limit of the more general models we studied previously [7]. We also assume that the fermions derive their weak properties from two adjacent  $SU(2)$  groups in the deconstructed model – *i.e.*, we consider “one-site” delocalization.

We have found several relationships between delocalization and electroweak corrections, some confirming what has been found in the continuum and others entirely new. We confirm that it is possible for the value of the electroweak parameter  $\alpha S$  to be small in models including fermion delocalization; this has been shown already in the continuum [31, 32]. By working in the deconstructed limit, we may directly evaluate the size of electroweak corrections away from the  $Z$ -peak which arise from the exchange of Kaluza-Klein modes; this has not previously been examined in the continuum. The size of these corrections is summarized by the electroweak parameter  $\alpha\delta$  [9, 12], which describes flavor-universal non-oblique corrections. In one-site delocalized Higgsless models with small values of  $\alpha S$ , we show that the amount of delocalization is bounded from above by a combination of experimental limits on  $\alpha\delta$  and the need to ensure that the scattering of longitudinal  $W$  bosons is properly unitarized. At 95% CL, the amount of delocalization cannot exceed 25%. We discuss the relation of these calculations to our previous calculations in deconstructed Higgsless models, and to models of extended technicolor. We defer to a subsequent work [33] the study of multi-site or flavor non-universal delocalization, and the generation of fermion masses.

In the next two sections we discuss the structure of the gauge and fermion sectors of the model, and specify the limit in which we analytically compute the size of corrections to electroweak interactions. In sections 4, 5, and 6, we compute the electroweak parameters  $\alpha S$ ,  $\alpha T$ , and  $\alpha\delta$ , respectively.\* In section 7 we discuss the interpretation of these models, and discuss how such effects can arise in technicolor theories. In section 8 we present numerical results for a four-site model, illustrating our analytic calculations and demonstrating explicitly that some models with vanishing  $\alpha S$  can have relatively large values of  $\alpha\delta$ . Section 9 discusses our conclusions and outlines future work.

## 2. Review of the Gauge Sector of the Model

We study a deconstructed Higgsless model, as shown diagrammatically (using “moose notation” [34]) in Figure 1. The model incorporates an  $SU(2)^{N+1} \times U(1)$  gauge group, and  $N + 1$  nonlinear  $(SU(2) \times SU(2))/SU(2)$  sigma models in which the global symmetry groups in adjacent sigma models are identified with the corresponding factors of the gauge group. The Lagrangian for this model to leading order is given by

$$\mathcal{L}_2 = \frac{1}{4} \sum_{j=1}^{N+1} f_j^2 \text{tr} \left( (D_\mu U_j)^\dagger (D^\mu U_j) \right) - \sum_{j=0}^{N+1} \frac{1}{2g_j^2} \text{tr} (F_{\mu\nu}^j F^{j\mu\nu}), \quad (2.1)$$

---

\*The fourth such parameter,  $\Delta\rho$ , is identically equal to 0 in Case I models [7].



$m_{W0}^2$  are, respectively, identified as the usual  $Z$  and  $W$  bosons. We will generally refer to these last eigenvalues by their conventional symbols  $M_Z^2$ ,  $M_W^2$ ; the distinction between these and the corresponding mass matrices should be clear from context.

Generalizing the usual mathematical notation for “open” and “closed” intervals, we may denote [7] the neutral-boson mass matrix  $M_Z^2$  as  $M_{[0,N+1]}^2$  — *i.e.*, it is the mass matrix for the entire moose running from site 0 to site  $N + 1$  including the gauge couplings of both endpoint groups. Analogously, the charged-boson mass matrix  $M_W^2$  is  $M_{[0,N+1]}^2$  — it is the mass matrix for the moose running from site 0 to link  $N + 1$ , but not including the gauge coupling at site  $N + 1$ . This notation will be useful in thinking about the properties of sub-matrices  $M_{[0,i]}^2$  of the full gauge-boson mass matrices that arise in our discussion of fermion delocalization, and also the corresponding eigenvalues  $m_{i\hat{i}}^2$  ( $\hat{i} = 1, 2, \dots, i$ ). We will denote the lightest such eigenvalue  $m_{i1}^2$  by the symbol  $M_i^2$ .

### 3. A Moose with Delocalized Fermions

Consider the simplest deconstructed Higgsless model with one-site delocalized fermions, as shown in Figure 1. We take the fermion couplings in this model to be

$$\mathcal{L}_f = \bar{J}_L^\mu \cdot (x_0 A_\mu^0 + x_1 A_\mu^1) + J_Y^\mu A_\mu^{N+1} , \quad (3.1)$$

where  $x_0 + x_1 = 1$  and the fermions are “delocalized” in the sense that their  $SU(2)$ -couplings arise from both sites 0 and 1. Note that the fermion couplings are flavor universal. This expression is not separately gauge invariant under  $SU(2)_0$  and  $SU(2)_1$ . Rather, as discussed further in section 7, eqn. (3.1) should be viewed as the form of the fermion coupling in “unitary” gauge. Here  $\bar{J}_L^\mu$  denotes the isotriplet of left-handed weak fermion currents, and  $J_Y^\mu$  is the fermion hypercharge current. In the notation of reference [7], where the fermion coupled to the  $SU(2)$  group at site  $p$ , the current model is an admixture of  $p = 0$  and  $p = 1$ . As we will see, our results for the electroweak parameters in this model are themselves an admixture of the results we would obtain in the two models.<sup>†</sup>

Because fermions are charged under  $SU(2)$  gauge groups at sites 0 and 1, as well as under the single  $U(1)$  group at the  $N + 1$  site, neutral current four-fermion processes may be derived from the Lagrangian

$$\begin{aligned} \mathcal{L}_{nc} = & -\frac{1}{2} \left[ \sum_{i,j=0}^1 x_i x_j g_i g_j D_{i,j}^Z(Q^2) \right] J_3^\mu J_{3\mu} - \left[ \sum_{i=0}^1 x_i g_i g_{N+1} D_{i,N+1}^Z(Q^2) \right] J_3^\mu J_{Y\mu} \\ & - \frac{1}{2} [g_{N+1}^2 D_{N+1,N+1}^Z(Q^2)] J_Y^\mu J_{Y\mu} , \end{aligned} \quad (3.2)$$

---

<sup>†</sup>The idea of a delocalized model as an admixture of localized-fermion models corresponding to different values of  $p$  generalizes readily to multi-site delocalization. The generalization of the form of equations (3.1) - (3.7) is obvious; the implications will be discussed in a forthcoming paper. [33]

and charged-current process from

$$\mathcal{L}_{cc} = -\frac{1}{2} \left[ \sum_{i,j=0}^1 x_i x_j g_i g_j D_{i,j}^W(Q^2) \right] J_+^\mu J_{-\mu} . \quad (3.3)$$

where  $D_{i,j}$  is the  $(i,j)$  element of the appropriate gauge field propagator matrix. We can define correlation functions between fermion currents at given sites as

$$[G_{NC}(Q^2)]_{i,j} = g_i g_j D_{i,j}^Z(Q^2) \quad [G_{CC}(Q^2)]_{i,j} = g_i g_j D_{i,j}^W(Q^2) . \quad (3.4)$$

The full correlation function for the fermion currents  $J_3^\mu$  and  $J_Y^\mu$  is then

$$[G_{NC}(Q^2)]_{WY} = \sum_{i=0}^1 x_i [G_{NC}(Q^2)]_{i,N+1} , \quad (3.5)$$

where we have used eqn. (3.1) to include the appropriate contribution from each site to which fermions couple. Likewise, the full correlation function for weak currents is

$$[G_{NC,CC}]_{WW} = \sum_{i,j=0}^1 x_i x_j [G_{NC,CC}]_{i,j} . \quad (3.6)$$

The hypercharge correlation function  $[G_{NC}(Q^2)]_{YY} = [G_{NC}(Q^2)]_{N+1,N+1}$  depends only on the single site with a  $U(1)$  gauge group.

The correlation functions may be written in a spectral decomposition in terms of the mass eigenstates as follows:

$$[G_{NC}(Q^2)]_{YY} = \frac{[\xi_\gamma]_{YY}}{Q^2} + \frac{[\xi_Z]_{YY}}{Q^2 + M_Z^2} + \sum_{z=1}^N \frac{[\xi_{Zz}]_{YY}}{Q^2 + m_{Zz}^2} , \quad (3.7)$$

$$[G_{NC}(Q^2)]_{WY} = \frac{[\xi_\gamma]_{WY}}{Q^2} + \frac{[\xi_Z]_{WY}}{Q^2 + M_Z^2} + \sum_{z=1}^N \frac{[\xi_{Zz}]_{WY}}{Q^2 + m_{Zz}^2} , \quad (3.8)$$

$$[G_{NC}(Q^2)]_{WW} = \frac{[\xi_\gamma]_{WW}}{Q^2} + \frac{[\xi_Z]_{WW}}{Q^2 + M_Z^2} + \sum_{z=1}^N \frac{[\xi_{Zz}]_{WW}}{Q^2 + m_{Zz}^2} , \quad (3.9)$$

$$[G_{CC}(Q^2)]_{WW} = \frac{[\xi_W]_{WW}}{Q^2 + M_W^2} + \sum_{w=1}^N \frac{[\xi_{Ww}]_{WW}}{Q^2 + m_{Ww}^2} , \quad (3.10)$$

All poles should be simple (i.e. there should be no degenerate mass eigenvalues) because, in the continuum limit, we are analyzing a self-adjoint operator on a finite interval. Since the neutral bosons couple to only two currents,  $J_3^\mu$  and  $J_Y^\mu$ , the three sets of residues in equations (3.7)–(3.8) must be related. Specifically, they satisfy the  $N + 1$  consistency conditions,

$$[\xi_Z]_{WW} [\xi_Z]_{YY} = ([\xi_Z]_{WY})^2 , \quad [\xi_{Zz}]_{WW} [\xi_{Zz}]_{YY} = ([\xi_{Zz}]_{WY})^2 . \quad (3.11)$$

In the case of the photon, charge universality further implies

$$e^2 = [\xi_\gamma]_{WW} = [\xi_\gamma]_{WY} = [\xi_\gamma]_{YY} . \quad (3.12)$$

### 3.1 Notation

We will find it useful to define the following sums over heavy eigenvalues for phenomenological discussions:

$$\Sigma_{(i,j)} \equiv \text{Tr } M_{(i,j)}^{-2} \quad (3.13)$$

with similar definitions for  $\Sigma_{[i,j]}$  and so on. In particular,

$$\Sigma_Z \equiv \sum_{z=1}^N \frac{1}{m_{Zz}^2}, \quad \Sigma_W \equiv \sum_{w=1}^N \frac{1}{m_{Ww}^2}; \quad (3.14)$$

that is,  $\Sigma_Z$  and  $\Sigma_W$  are the sums over inverse-square masses of the higher neutral- and charged-current KK modes of the full model. Furthermore, by explicit calculation one finds (see Appendix B of Ref. [7])

$$\Sigma_{(0,N+1)} = \sum_{i=1}^N \frac{4F^2}{g_i^2 F_i^2 \tilde{F}_i^2}, \quad (3.15)$$

where

$$\frac{1}{F_i^2} = \sum_{j=i+1}^{N+1} \frac{1}{f_j^2}, \quad \frac{1}{\tilde{F}_i^2} = \sum_{j=1}^i \frac{1}{f_j^2}, \quad (3.16)$$

and  $F_0^2 = \tilde{F}_{N+1}^2 = F^2$ .

Finally, we will find it useful to denote the (0,0) element of the gauge boson mass matrices as

$$[M_Z^2]_{0,0} = [M_W^2]_{0,0} = \frac{g_0^2 f_1^2}{4} \equiv \tilde{m}^2. \quad (3.17)$$

To connect with the notation of Ref. [7] we note that

$$\tilde{m}^{-2} = \Sigma_{[0,1]} \equiv \Sigma_{p=1} \quad (3.18)$$

### 3.2 Electroweak Parameters

As we have shown in [9], the most general amplitude (to leading order in deviation from the standard model) for low-energy four-fermion neutral weak current processes in any ‘‘universal’’ model [12] may be written as<sup>‡</sup>

$$\begin{aligned} -\mathcal{M}_{NC} = e^2 \frac{\mathcal{Q}\mathcal{Q}'}{Q^2} + & \frac{(I_3 - s^2\mathcal{Q})(I_3' - s^2\mathcal{Q}')}{\left(\frac{s^2c^2}{e^2} - \frac{S}{16\pi}\right)Q^2 + \frac{1}{4\sqrt{2}G_F} \left(1 - \alpha T + \frac{\alpha\delta}{4s^2c^2}\right)} \\ & + \sqrt{2}G_F \frac{\alpha\delta}{s^2c^2} I_3 I_3' + 4\sqrt{2}G_F (\Delta\rho - \alpha T) (\mathcal{Q} - I_3)(\mathcal{Q}' - I_3'), \end{aligned} \quad (3.19)$$

---

<sup>‡</sup>See [9] for a discussion of the correspondence between the ‘‘on-shell’’ parameters defined here, and the zero-momentum parameters defined in [12]. Note that  $U$  is shown in [9] to be zero to the order we consider in this paper.

and the matrix element for charged current process may be written

$$-\mathcal{M}_{\text{CC}} = \frac{(I_+ I'_- + I_- I'_+)/2}{\left(\frac{s^2}{e^2} - \frac{S}{16\pi}\right) Q^2 + \frac{1}{4\sqrt{2}G_F} \left(1 + \frac{\alpha\delta}{4s^2c^2}\right)} + \sqrt{2}G_F \frac{\alpha\delta}{s^2c^2} \frac{(I_+ I'_- + I_- I'_+)}{2}. \quad (3.20)$$

Note that the parameter  $s^2$  is defined implicitly in these expressions as the ratio of the  $\mathcal{Q}$  and  $I_3$  couplings of the  $Z$  boson.  $S$  and  $T$  are the familiar oblique electroweak parameters [35, 36, 37], as determined by examining the *on-shell* properties of the  $Z$  and  $W$  bosons.  $\Delta\rho$  corresponds to the deviation from unity of the ratio of the strengths of low-energy isotriplet weak neutral-current scattering and charged-current scattering. Finally, the contact interactions proportional to  $\alpha\delta$  and  $(\Delta\rho - \alpha T)$  correspond to “universal non-oblique” corrections.

From our previous analysis [7], we know that for a model of the sort shown in Figure 1,  $\Delta\rho \equiv 0$ . In the limit in which we will work (see eqns. (3.22) and (3.23)), we will also find (Section 5) that  $\alpha T \approx 0$ . Therefore our analysis of electroweak corrections in these models reduces to computing the values of  $\alpha S$  and  $\alpha\delta$ .

### 3.3 The Limit Taken

We will study the correlation functions for  $0 \leq -Q^2 \leq (200 \text{ GeV})^2$  at tree-level assuming that the heavy  $W$ - and  $Z$ -bosons satisfy

$$m_{Zz}^2, m_{Ww}^2 \gg (200 \text{ GeV})^2. \quad [z, w = 1, \dots, N] \quad (3.21)$$

From our previous analysis [7], we expect that  $g_{N+1}$  (being the only  $U(1)$  coupling) must be smaller than the other  $g_i$  in order to ensure that a light  $Z$  state will exist. In principle, any one of the  $SU(2)$  couplings could also be small (to ensure the presence of a light  $W$ ). However, our previous analysis [7] tells us that, in a viable model, any site with small coupling must be linked by large  $f$ -constants to site 0. For simplicity, we will therefore restrict our attention to the case where the only  $SU(2)$  site with a small coupling is site 0. This may be viewed as analyzing the general model after having “integrated out” the links with large  $f$ -constants.

In our analytic work, therefore, we will work in the limit that

$$g_0, g_{N+1} \ll g_i, \quad i = 1, \dots, N. \quad (3.22)$$

From the analyses presented in [7], we find that in the the limit of eqn. (3.22),

$$\Sigma_Z \approx \Sigma_W \approx \Sigma_{(0,N+1)} \equiv \Sigma_r, \quad (3.23)$$

where the last definition makes contact with the notation  $M_{(0,N+1)}^2 \equiv M_r^2$  in Ref. [7], and

$$M_W^2 = \frac{g_0^2 F^2}{4} + \mathcal{O}\left(\frac{M_W^2}{m_{W1}^2}\right). \quad (3.24)$$

Note that we expect  $g_0$  to be approximately of order the standard model  $SU(2)$  coupling and therefore numerically of order 1 – the limit in eqn. (3.22) implies that the other  $g_i$  will be larger, and eqn. (3.24) implies that  $F \simeq 246$  GeV.

For phenomenologically motivated reasons (see eqn. (4.12)), we will also take

$$x_1 \frac{\{-Q^2, M_W^2\}}{\tilde{m}^2} \ll 1 . \quad (3.25)$$

This approximation may be satisfied either by  $x_1$  being small,  $\tilde{m}^2$  being large, or some combination thereof.

In the numerical examples studied in Section 8, we calculate the tree-level masses and residues exactly, and we confirm that our analytic calculations based on the approximations of eqn. (3.22) and (3.25) do indeed capture the essential features of models with one-site delocalization.

#### 4. $[G_{NC}(Q^2)]_{WY}$ , $[\xi_Z]_{WY}$ and $\alpha S$

We begin by computing  $[G_{NC}(Q^2)]_{WY}$ . Starting from eqn. (3.5), we see the two contributions coming from the two sites at which the fermion resides. Based on Ref. [7], then, we may immediately compute the the two relevant elements of the propagator matrix

$$\begin{aligned} [G_{NC}(Q^2)]_{0,N+1} &= \frac{e^2 M_Z^2}{Q^2(Q^2 + M_Z^2)} \left[ \prod_{z=1}^N \frac{m_{Zz}^2}{Q^2 + m_{Zz}^2} \right] \\ [G_{NC}(Q^2)]_{1,N+1} &= \frac{e^2 M_Z^2}{Q^2(Q^2 + M_Z^2)} \left[ \frac{Q^2 + \tilde{m}^2}{\tilde{m}^2} \right] \left[ \prod_{z=1}^N \frac{m_{Zz}^2}{Q^2 + m_{Zz}^2} \right] . \end{aligned} \quad (4.1)$$

Combining these results, we find

$$[G_{NC}(Q^2)]_{WY} = \frac{e^2 M_Z^2}{Q^2(Q^2 + M_Z^2)} \left[ 1 + x_1 \frac{Q^2}{\tilde{m}^2} \right] \left[ \prod_{z=1}^N \frac{m_{Zz}^2}{Q^2 + m_{Zz}^2} \right] . \quad (4.2)$$

Given eqns. (3.21) and (3.25), we may expand the final product in this expression and find

$$[G_{NC}(Q^2)]_{WY} = \frac{e^2 M_Z^2}{Q^2(Q^2 + M_Z^2)} \left[ 1 + Q^2 \left( \frac{x_1}{\tilde{m}^2} - \Sigma_Z \right) \right] . \quad (4.3)$$

If we take

$$x_1 = \frac{\Sigma_Z}{\Sigma_{[0,1]}} = \tilde{m}^2 \Sigma_Z . \quad (4.4)$$

we have that (in this momentum range) this correlation function equals its standard model value to leading order,

$$[G_{NC}(Q^2)]_{WW} \equiv [G_{NC}(Q^2)]_{WW}^{SM} . \quad (4.5)$$

Next, we compute  $[\xi_Z]_{WY}$ , from which we may directly extract  $\alpha S$ . The residue decomposes like the correlation function

$$[\xi_Z]_{WY} = x_0[\xi_Z]_{0,N+1} + x_1[\xi_Z]_{1,N+1} , \quad (4.6)$$

where the subscripts on the right hand side of the equation denote the residue of the pole of the corresponding propagator matrix element. From eqn. (4.1), we find

$$\begin{aligned} [\xi_Z]_{0,N+1} &= -e^2[1 + M_Z^2 \Sigma_Z] \\ [\xi_Z]_{1,N+1} &= -e^2[1 + M_Z^2(\Sigma_Z - \Sigma_{[0,1]})] . \end{aligned} \quad (4.7)$$

Combining these results, we find

$$[\xi_Z]_{WY} = -e^2[1 + M_Z^2(\Sigma_Z - x_1 \Sigma_{[0,1]})] . \quad (4.8)$$

The form of the four-fermion weak interaction amplitudes of eqns. (3.19) and (3.20) implies [7]

$$\frac{1}{e^2}[\xi_Z]_{WY} = -1 - \frac{\alpha}{4s_Z^2 c_Z^2} S , \quad (4.9)$$

and hence we find

$$\alpha S = 4s_Z^2 c_Z^2 M_Z^2 (\Sigma_Z - x_1 \tilde{m}^{-2}) . \quad (4.10)$$

Now it is clear that the same ‘‘tuning’’ of the localization of the fermion in conjunction with the heavy  $Z$ -boson mass matrix that causes  $[G_{NC}(Q^2)]_{WY}$  to have its standard model form at low momentum likewise makes  $\alpha S$  small. In fact, if equation (4.4) is satisfied, then  $\alpha S \simeq 0$

Using eqn. (3.18), we may rewrite this result in the form

$$\alpha S = 4s_Z^2 c_Z^2 M_Z^2 (\Sigma_Z - x_1 \Sigma_{p=1}) , \quad (4.11)$$

which agrees with the results of [7] when  $x_0 = 1$  or  $x_1 = 1$ , and smoothly interpolates between these extremes.

Finally, note that, in order for  $\alpha S$  to be small, we need

$$x_1 \frac{M_W^2}{\tilde{m}^2} = M_W^2 \Sigma_Z \ll 1 , \quad (4.12)$$

and the limit of eqn. (3.25) is directly related to that of eqn. (3.21).

## 5. $[G_{NC}(Q^2)]_{YY}$ , $[\xi_Z]_{YY}$ and $\alpha T$

Next, consider the correlation function  $[G_{NC}(Q^2)]_{YY}$ . Given the structure of the moose in Figure 1 and the form of the fermion couplings in eqn. (3.1), we see that the delocalization of the fermions is irrelevant in this case – we get the same result [7] as in the case of the simplest case I model:

$$[G_{NC}(Q^2)]_{YY} = \frac{e^2 M_Z^2 (Q^2 + M_W^2)}{Q^2 M_W^2 (Q^2 + M_Z^2)} \left[ \prod_{w=1}^N \frac{Q^2 + m_{Ww}^2}{m_{Ww}^2} \right] \left[ \prod_{z=1}^N \frac{m_{Zz}^2}{Q^2 + m_{Zz}^2} \right] . \quad (5.1)$$

Expanding for low  $Q^2$  (see eqn. (3.21)) we find, to this order,

$$[G_{NC}(Q^2)]_{YY} = \frac{e^2 M_Z^2 (Q^2 + M_W^2)}{Q^2 M_W^2 (Q^2 + M_Z^2)} [1 + Q^2 (\Sigma_W - \Sigma_Z)] = [G_{NC}(Q^2)]_{YY}^{SM} . \quad (5.2)$$

where the last equality follows from eqn. (3.23) and where  $G_{NC}(Q^2)]_{YY}^{SM}$  denotes the tree-level standard model value in terms of  $e^2$ ,  $M_W^2$ , and  $M_Z^2$ .

The residue is likewise the same as in the simplest Case I model:

$$[\xi_Z]_{YY} = \frac{e^2 (M_Z^2 - M_W^2)}{M_W^2} [1 + M_Z^2 (\Sigma_Z - \Sigma_W)] . \quad (5.3)$$

Therefore, using the results of [7], we find

$$\alpha T = s_Z^2 M_Z^2 (\Sigma_Z - \Sigma_W) \simeq 0 , \quad (5.4)$$

independent of the value of  $x_0$ . The last equality follows from eqn. (3.23) (i.e. from working in the limit  $g_{N+1}^2 \ll 1$ ).

## 6. $[G_{CC}(Q^2)]_{ww}$ , $[\xi_w]_{ww}$ , and $\alpha\delta$

Finally, to compute  $\alpha\delta$  we must compute a  $WW$  correlation function. For simplicity, we will consider the charged-current correlation function  $[G_{CC}(Q^2)]_{WW}$ . We may do so by recalling that the matrix  $G_{CC}(Q^2)$  is defined by

$$[G_{CC}(Q^2)]_{i,j} \equiv g_i g_j [(Q^2 + M_W^2)^{-1}]_{i,j} . \quad (6.1)$$

The correlation function of  $J_\mu^+$  with  $J_\nu^-$  is therefore proportional to

$$x_0^2 [G_{CC}(Q^2)]_{0,0} + 2x_0 x_1 [G_{CC}(Q^2)]_{0,1} + x_1^2 [G_{CC}(Q^2)]_{1,1} . \quad (6.2)$$

To make progress, we relate the various propagator elements to one another. Consider eqn. (6.1) as a matrix equation

$$G_{CC}(Q^2) = G \cdot \frac{\mathcal{I}}{Q^2 + M_W^2} \cdot G , \quad (6.3)$$

where  $G$  is the matrix of gauge coupling constants, and where  $\mathcal{I}$  denotes the identity matrix in gauge space. From this, we immediately see that we have the matrix relation

$$(Q^2 + M_W^2) \cdot G^{-1} \cdot G_{CC}(Q^2) \cdot G^{-1} \equiv \mathcal{I} . \quad (6.4)$$

Applying this relation explicitly to the first row of the matrix  $(Q^2 + M_W^2)$  and the first two columns of the matrix  $G_{CC}(Q^2)$ , we find the relations<sup>§</sup>

$$[G_{CC}(Q^2)]_{0,1} = \frac{\tilde{m}^2}{Q^2 + \tilde{m}^2} [G_{CC}(Q^2)]_{1,1} , \quad (6.5)$$

---

<sup>§</sup>The propagator matrix elements  $[G_{CC}(Q^2)]_{0,1}$  and  $[G_{CC}(Q^2)]_{0,0}$  do not have poles at  $Q^2 = -\tilde{m}^2$ , as might be inferred from the form of eqns. (6.5) and (6.6). Rather, these potential poles are cancelled by zeros of the numerators in these expressions.

and

$$[G_{CC}(Q^2)]_{0,0} = \frac{g_0^2 \left(1 + \frac{f_1^2}{4} [G_{CC}(Q^2)]_{0,1}\right)}{Q^2 + \tilde{m}^2}. \quad (6.6)$$

Using these results, we find

$$[G_{CC}(Q^2)]_{WW} = \left(1 + x_1 \frac{Q^2}{\tilde{m}^2}\right)^2 [G_{CC}(Q^2)]_{0,0} - \frac{8x_1}{f_1^2} + \frac{4x_1^2}{f_1^2} \left(1 - \frac{Q^2}{\tilde{m}^2}\right). \quad (6.7)$$

Combining the limit of eqn. (3.25) with eqns. (3.17) and (3.24), we see that

$$\frac{(-Q^2)x_1}{f_1^2} \approx \frac{(-Q^2)}{F^2} \left(x_1 \frac{M_W^2}{\tilde{m}^2}\right) \ll 1. \quad (6.8)$$

Hence, for the momenta of interest, eqn. (6.7) reduces to

$$[G_{CC}(Q^2)]_{WW} = \left(1 + 2x_1 \frac{Q^2}{\tilde{m}^2}\right) [G_{CC}(Q^2)]_{0,0} - \frac{8x_1}{f_1^2} + \frac{4x_1^2}{f_1^2}. \quad (6.9)$$

We can re-arrange this to isolate the pole at  $Q^2 = -M_W^2$  from the non-pole pieces of the correlation function:

$$\begin{aligned} [G_{CC}(Q^2)]_{WW} &= \left(1 - 2x_1 \frac{M_W^2}{\tilde{m}^2}\right) [G_{CC}(Q^2)]_{0,0} + \frac{2x_1}{\tilde{m}^2} (Q^2 + M_W^2) [G_{CC}(Q^2)]_{0,0} \\ &\quad - \frac{4x_1}{F^2} \left(\frac{M_W^2}{\tilde{m}^2}\right) (2 - x_1), \end{aligned} \quad (6.10)$$

where we have used eqn. (3.24) to simplify the last term.

From the pole term (first term) of eqn. (6.10) we see that the residue of the charged-current correlation function at  $Q^2 = -M_W^2$  is

$$[\xi_W]_{WW} = \left(1 - 2x_1 \frac{M_W^2}{\tilde{m}^2}\right) [\xi_W]_{0,0}. \quad (6.11)$$

Applying the calculations presented in [7], we observe that

$$[\xi_W]_{0,0} = \frac{e^2 M_Z^2}{M_Z^2 - M_W^2} [1 + M_W^2 (\Sigma_Z + \Sigma_W)] = [\xi_W]^{SM} [1 + 2M_W^2 \Sigma_Z], \quad (6.12)$$

where the last equality follows from eqn. (3.23), and  $[\xi_W]^{SM}$  denotes the tree-level standard model value of the residue expressed in terms of  $M_{W,Z}^2$ . Therefore, we find from eqn. (6.11) that

$$[\xi_W]_{WW} = \left(1 - 2x_1 \frac{M_W^2}{\tilde{m}^2} + 2M_W^2 \Sigma_Z\right) [\xi_W]^{SM} \quad (6.13)$$

For  $x_1 = \tilde{m}^2 \Sigma_Z$  (i.e., for  $\alpha S = 0$ ), the residue of the pole equals the standard model value. This is consistent with the form of eqn. (3.20).

While the residue of the  $W$ -pole is given by its standard model value, the non-pole terms in eqn. (6.10) give rise to a non-zero value of  $\alpha\delta$ . From the analyses presented in [7],

$$[G_{CC}(Q^2)]_{0,0} = \frac{4M_W^2}{F^2[Q^2 + M_W^2]} \left[ \prod_{w=1}^N \frac{m_{Ww}^2}{Q^2 + m_{Ww}^2} \right] \left[ \prod_{r=1}^N \frac{Q^2 + m_r^2}{m_r^2} \right]. \quad (6.14)$$

Expanding the product for the momenta of interest, this may be written

$$[G_{CC}(Q^2)]_{0,0} = \frac{4M_W^2}{F^2[Q^2 + M_W^2]} [1 + Q^2(\Sigma_r - \Sigma_W)] \approx \frac{4M_W^2}{F^2[Q^2 + M_W^2]}, \quad (6.15)$$

where the last equality follows from eqn. (3.23). Comparing the non-pole terms in eqn. (6.10) with the form of the matrix element eqn. (3.20), we therefore calculate

$$\sqrt{2}G_F \frac{\alpha\delta}{s^2c^2} = \frac{4x_1^2}{F^2} \left( \frac{M_W^2}{\tilde{m}^2} \right). \quad (6.16)$$

However,

$$\sqrt{2}G_F \equiv \frac{1}{4}[G_{CC}(Q^2 = 0)]_{WW} \quad (6.17)$$

so from eqn. (6.9), again using eqns. (3.17) and (3.24), we see that

$$\sqrt{2}G_F = \frac{1}{F^2} - \frac{(2-x_1)x_1}{f_1^2} \approx \frac{1}{F^2} \left[ 1 - \frac{(2-x_1)x_1 M_W^2}{\tilde{m}^2} \right] = \frac{1}{F^2} \left[ 1 + \mathcal{O}\left(\frac{x_1 M_W^2}{\tilde{m}^2}\right) \right] \quad (6.18)$$

Using this in eqn. (6.16) we find

$$\frac{\alpha\delta}{4s^2c^2} = x_1^2 \frac{M_W^2}{\tilde{m}^2} \quad (6.19)$$

If we employ eqn. (3.18), this can be rewritten as

$$\frac{\alpha\delta}{4s^2c^2} = x_1^2 M_W^2 \Sigma_{p=1}, \quad (6.20)$$

which agrees with the results of [7] for  $x_0 = 1$  or  $x_1 = 1$  and smoothly interpolates between them.

When we choose the amount of delocalization to ensure that  $\alpha S$  vanishes,  $x_1 = \tilde{m}^2 \Sigma_Z$ , we find

$$\frac{\alpha\delta}{4s^2c^2} = x_1 M_W^2 \Sigma_Z. \quad (6.21)$$

Moreover, as argued previously [7], preserving the unitarity of longitudinal  $W$  boson scattering requires that  $M_W^2 \Sigma_Z \geq 4 \times 10^{-3}$ . The results of [12] imply<sup>¶</sup> that experiment currently imposes the upper bound  $\alpha\delta/4s^2c^2 < 1 \times 10^{-3}$  at 95% CL. Hence we must have

$$x_1 \leq \frac{1}{4}, \quad (6.22)$$

and the amount of delocalization is bounded to be less than of order 25%.

---

<sup>¶</sup>When  $\alpha S = 0 = (\Delta\rho - \alpha T)$ , from eqn. (1.1) we see that  $\hat{S} = \alpha\delta/4s^2c^2$ .

## 7. Beyond Extra Dimensions

### 7.1 Re-interpreting fermion delocalization

The “delocalized” fermion coupling in deconstructed Higgsless models, eqn. (3.1), may also be written using the Goldstone boson fields of the Moose in Figure 1. Consider the current operator

$$\text{Tr} \left( \frac{\sigma^a}{2} U_1^\dagger i D_\mu U_1 \right) \rightarrow +\frac{1}{2} (A_{0\mu}^a - A_{1\mu}^a) , \quad (7.1)$$

where the  $\sigma$  are the Pauli matrices,  $D_\mu$  is the covariant derivative

$$i D_\mu U_1 = i \partial_\mu U_1 + \frac{\vec{A}_{0\mu} \cdot \vec{\sigma}}{2} U_1 - U_1 \frac{\vec{A}_{1\mu} \cdot \vec{\sigma}}{2} , \quad (7.2)$$

consistent with eqn. (3.1), and where we have specified the form of this operator in unitary gauge, where all the link fields  $U_j \equiv \mathcal{I}$ . In this language, we see that the fermions’ weak couplings in eqn. (3.1) may be written

$$\vec{J}_L^\mu \cdot \left[ \vec{A}_\mu^0 - 2x_1 \text{Tr} \left( \frac{\vec{\sigma}}{2} U_1^\dagger i D_\mu U_1 \right) \right] . \quad (7.3)$$

From this point of view, the fermions are charged only under  $SU(2)_0$  and the apparent delocalization comes about from couplings to the Goldstone-boson fields.<sup>||</sup>

Note that, in the gauge-boson normalization we are using, the linear combination of gauge fields  $A_{0\mu}^a - A_{1\mu}^a$  are strictly orthogonal to the photon

$$A_\mu^\gamma \propto A_{0\mu}^3 + A_{1\mu}^3 + \dots + A_{N+1\mu}^3 . \quad (7.4)$$

Hence, the couplings of eqn. (7.3) result in a modification of the  $Z$  and  $W$ -couplings whose size depends on the  $x_1$  and the admixture of  $A_0 - A_1$  in the mass-eigenstate  $W$  and  $Z$  fields. *But the couplings of eqn. (7.3) do not modify the photon coupling.*

### 7.2 Technicolor

We have seen that fermion delocalization, on the one hand, affects  $\alpha S$ , and, on the other, can be rewritten as the fermions coupling to the Goldstone boson currents. We can apply the idea of fermions’ coupling to Goldstone bosons directly to technicolor – a two-site model – which has no extra-dimensional interpretation. Consider the two-site model of Figure 2, with fermion couplings\*\*

$$\mathcal{L}_f = \vec{J}_L^\mu \cdot \left[ \vec{A}_\mu^0 - 2x_1 \text{Tr} \left( \Sigma^\dagger \frac{\vec{\sigma}}{2} i D_\mu \Sigma \right) \right] + J_Y^\mu A_\mu^1 , \quad (7.5)$$

---

<sup>||</sup>This also generalizes naturally to models with multi-site delocalization.

<sup>\*\*</sup>This kind of operator was previously considered in references [38, 39, 40, 41], the first of these prior to the definition of  $\alpha S$  and the last considering only flavor-dependent effects. Note that there is only one  $SU(2)$  group.

where  $\Sigma$  is the unitary matrix representing the three eaten Goldstone bosons, and the  $\vec{\sigma}$  are the Pauli matrices. Following [41], we find that in unitary gauge

$$2x_1 \vec{J}_L^\mu \cdot \text{Tr} \left( \Sigma^\dagger \frac{\vec{\sigma}}{2} iD_\mu \Sigma \right) \rightarrow -2x_1 \left[ \frac{e}{\tilde{s}\tilde{c}} Z^\mu J_\mu^3 + \frac{e}{\tilde{s}\sqrt{2}} (W^{+\mu} J_\mu^- + W^{-\mu} J_\mu^+) \right], \quad (7.6)$$

where

$$g_0 = \frac{e}{\tilde{s}}, \quad g_1 = \frac{e}{\tilde{c}}. \quad (7.7)$$

Hence, we find the overall  $Z$  and  $W$  couplings

$$\frac{e}{\tilde{s}\tilde{c}} Z^\mu [(1 - 2x_1) J_\mu^3 - \tilde{s}^2 J_\mu^Q], \quad (7.8)$$

$$\frac{e}{\sqrt{2}\tilde{s}} (1 - 2x_1) [W^{+\mu} J_\mu^- + W^{-\mu} J_\mu^+]. \quad (7.9)$$

Comparing with eqns. (3.19) and (3.20) we find

$$\tilde{s}^2 = s^2(1 - 2x_1), \quad \alpha \Delta S \approx -8s^2 x_1, \quad (7.10)$$

As anticipated, the Goldstone-boson operator in eqn. (7.5) can shift  $\alpha S$ . In fact, it will shift  $\alpha S$  in a negative direction (since  $x_1$  is positive) just as occurs in eqn. (4.10).

In a technicolor model this effect could be used to cancel the positive QCD-size value of  $\alpha S$  arising [35, 42, 43] from the  $L_{10}$  operator. It is also amusing to note that the sign of  $x_1$  arising from the ETC operators considered in [41] is positive. If the operator of eqn. (7.5) arises from ETC exchange, that reference found (note that the convention for the covariant derivative differs in that reference)

$$x_1 = \frac{\xi^2 g_{ETC}^2 v^2}{4 M_{ETC}^2}, \quad (7.11)$$

where  $g_{ETC}$  and  $M_{ETC}$  are the extended technicolor coupling and gauge-boson mass,  $v \simeq 246$  GeV, and  $\xi$  is a model-dependent Clebsch-Gordon coefficient. The canonical QCD-like technicolor estimate gives  $S_{TC} = \mathcal{O}(0.5)$ . If we require the sum of the canonical contribution plus that arising from eqn. (7.10) to vanish, we find  $|x_1| \simeq 2 \times 10^{-3}$ , and hence

$$\frac{M_{ETC}}{\xi g_{ETC}} \simeq 3 \text{ TeV}. \quad (7.12)$$

In an ETC model, one would also expect contributions to  $\alpha\delta$  (from ETC exchange) of the same order – which implies there must be a Clebsch of order a few to suppress  $\alpha\delta$  relative to  $x_1$  [12]. One could imagine, for example, a model with flavor-independent left-handed low-scale ETC interactions (with light quark masses suppressed by high-scale right-handed interactions).

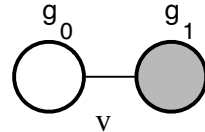


**Figure 2:** Simple two-site moose diagram corresponding to the global symmetry structure of the one-Higgs doublet standard model or the simplest one-doublet technicolor model.

## 8. Examples of Delocalized Deconstructed Higgsless Models

To illustrate the ideas discussed in the earlier sections of the paper, we now study a linear moose model with 4 sites and 3 links (Figure 3), a model small enough to be easily solved numerically without approximations. We will calculate the tree-level masses and residues exactly and confirm that our previous analytic calculations based on the approximations of eqn. (3.22) and (3.25) capture the essential features of models with one-site delocalization.

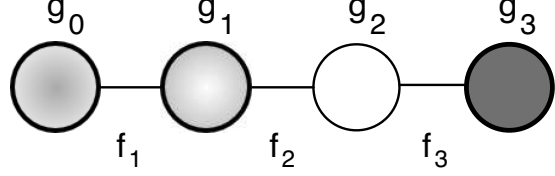


**Figure 3:** The model analyzed in the explicit numerical calculation. Sites 0 to 2 are  $SU(2)$  gauge groups, while site 3 is  $U(1)$ . Fermions are coupled to sites 0 and 1 (weak isospin), and to site 3 (weak hypercharge), as denoted by the thick circles.

Starting from this  $[SU(2)]^3 \times U(1)$  gauge structure, we introduce a chiral fermion  $\psi_{0L}$  (assumed to be a doublet of  $SU(2)_0$ ), and a Dirac fermion  $\psi_1 = \psi_{1L} + \psi_{1R}$  (doublet of  $SU(2)_1$ ). Both  $\psi_{0L}$  and  $\psi_1$  are assumed to have the same weak hypercharge  $Y_\psi$ . The fermion sector of this model is then given by the Lagrangian,

$$\begin{aligned} \mathcal{L}_{\text{fermion}} = & \bar{\psi}_{0L}(i\cancel{\partial} + \frac{\tau^a}{2}A_0^a + Y_\psi A_3)\psi_{0L} \\ & + \bar{\psi}_{1L}(i\cancel{\partial} + \frac{\tau^a}{2}A_1^a + Y_\psi A_3)\psi_{1L} + \bar{\psi}_{1R}(i\cancel{\partial} + \frac{\tau^a}{2}A_1^a + Y_\psi A_3)\psi_{1R}. \end{aligned} \quad (8.1)$$

The fermion mass term consistent with the gauge symmetry is given by

$$\mathcal{L}_{\text{mass}} = (\bar{\psi}_{0L}, \bar{\psi}_{1L}) \begin{pmatrix} y_\psi f_1 U_1 \\ M_\psi \end{pmatrix} \psi_{1R} + \text{h.c.} \quad (8.2)$$

After the gauge symmetry breaking,  $\psi_{1R}$  and

$$\psi_L^{(1)} = s_\psi \psi_{0L} + c_\psi \psi_{1L} \quad (8.3)$$

form a Dirac fermion and become massive; we identify this as a KK mode. There also remains a massless fermion

$$\psi_L^{(0)} = c_\psi \psi_{0L} - s_\psi \psi_{1L}, \quad (8.4)$$

where

$$c_\psi \equiv \frac{M_\psi}{\sqrt{y_\psi^2 f_1^2 + M_\psi^2}}, \quad s_\psi \equiv \frac{y_\psi f_1}{\sqrt{y_\psi^2 f_1^2 + M_\psi^2}}, \quad (8.5)$$

which we identify as the standard model fermion. Then  $\psi_L^{(0)}$  couples to the gauge fields as

$$\mathcal{L}_{\text{fermion}} = \bar{\psi}_L^{(0)}(i\cancel{\partial} + x_0 \frac{\tau^a}{2}A_0^a + x_1 \frac{\tau^a}{2}A_1^a + Y_\psi A_3)\psi_L^{(0)} + \dots, \quad (8.6)$$

where  $x_0 = c_\psi^2$  and  $x_1 = s_\psi^2$ .

In our phenomenological calculations, we use  $\alpha, G_F$ , and  $M_Z$  to specify the input parameters of the standard model. <sup>††</sup> The specific values used are [44]  $\alpha^{-1} = 128.91 \pm 0.02$ ,  $M_Z = 91.1876 \pm 0.0021$  GeV, and  $G_F = 1.16637 \times 10^{-5}$  GeV<sup>-2</sup>. The Weinberg angle in this scheme is defined by

$$s_Z^2 c_Z^2 \equiv \frac{e^2}{4\sqrt{2}G_F M_Z^2}, \quad c_Z^2 \equiv 1 - s_Z^2, \quad (8.7)$$

yielding  $s_Z^2 = 0.23108 \pm 0.00005$ .

Our 4-site linear moose model with one delocalized fermion can be specified by 8 parameters:  $f_i$  ( $i = 1, 2, 3$ ),  $g_i$  ( $i = 0, 1, 2, 3$ ) and  $x_1^2$ . Three combinations of these parameters have values set by the inputs  $\alpha, G_F$ , and  $M_Z$ . For instance,

$$\frac{1}{4\pi\alpha} = \sum_{i=0}^3 \frac{1}{g_i^2}, \quad (8.8)$$

and

$$4\sqrt{2}G_F = [G_{CC}(Q^2 = 0)]_{WW}, \quad (8.9)$$

where one applies eqn. (3.6) together with

$$[G_{CC}(Q^2 = 0)]_{0,0} = \sum_{i=1,2,3} \frac{4}{f_i^2}, \quad [G_{CC}(Q^2 = 0)]_{0,1} = [G_{CC}(Q^2 = 0)]_{1,1} = \sum_{i=2,3} \frac{4}{f_i^2}, \quad (8.10)$$

Requiring  $S = 0$  sets the value of one more combination, as in eqn. (4.12). In order to specify the remaining parameters, we adopt three ansatzes

$$f_2 = f_3, \quad g_1 = g_2 = 4. \quad (8.11)$$

The ansatz  $f_2 = f_3$  allows us to maximize the delay of the onset of unitarity violation in longitudinal  $W$  scattering. The large values of  $g_1$  and  $g_2$  are taken so as to push up the mass of the gauge-boson KK-modes. Combining the four requirements from  $(\alpha, G_F, M_Z, S)$  with the three ansatzes, only one free parameter, which we identify as  $f_1$ , is left in the 4-site model.

We have analyzed the 4-site model with three sample values of the single free parameter:  $f_1 = 300$  GeV (Set 1),  $f_1 = 1000$  (Set 2) and  $f_1 = 2000$  GeV (Set 3). Once  $f_1$  is chosen, the other  $f_i$ , the  $g_i$  and  $x_1$  have values given in the Table below, as set by the four inputs and three ansatzes. The masses listed as outputs in the Table were calculated by diagonalizing the gauge-boson mass-squared matrix numerically.

---

<sup>††</sup>Note that the tree level value of  $M_W$  in this scheme ( $M_W|_{\text{tree}} \equiv c_Z M_Z = 79.9607$  GeV) differs from the observed value ( $M_W|_{\text{exp}} = 80.425 \pm 0.038$  GeV), indicating the importance of one-loop radiative correction at 1% level. In this paper, however, we restrict ourselves to tree-level. We thus denote  $M_W^{\text{SM}} \equiv M_W|_{\text{tree}}$  in our calculations, and compare all correlation functions to the corresponding tree-level standard model results.

	Set 1	Set 2	Set 3
Inputs			
$f_1$	300 GeV	1000 GeV	2000 GeV
$f_2 = f_3$	591.850 GeV	356.303 GeV	348.922 GeV
$g_0$	0.657164	0.664421	0.663478
$g_1 = g_2$	4.0	4.0	4.0
$g_3$	0.357650	0.356505	0.356651
$x_1$	0.014771	0.139231	0.480892
Calculated Physical Masses			
$M_W$	79.9599 GeV	79.9486 GeV	79.9080 GeV
$m_{Z1}$	892.459 GeV	976.990 GeV	983.725 GeV
$m_{W1}$	888.827 GeV	975.913 GeV	982.737 GeV
$m_{Z2}$	1944.08 GeV	2162.17 GeV	4114.49 GeV
$m_{W2}$	1943.39 GeV	2162.17 GeV	4144.49 GeV

The calculated value of  $M_W$  in Sets 1 and 2 agrees with the tree level standard model value within the uncertainty of  $M_W|_{\text{exp}}$  about 0.038 GeV. Hence the measured value of  $M_W$  does not currently exclude either Set 1 or 2. The calculated value of  $M_W$  in Set 3 deviates from the tree level standard model value by about  $1.4\sigma$ ; Set 3 is therefore marginally excluded.

### 8.1 Correlation functions

To explore the expectations that the electroweak correlation functions will resemble their standard model counterparts at low momentum, we calculated their values over the LEP energy range  $\sqrt{-Q^2} = 90\text{--}200$  GeV, and compared the tree-level results in the moose model to the tree-level results in the standard model. We computed  $[G_{NC}(Q^2)]_{WY}$  for all three sets of parameters using expression (4.2) and found no discernible deviation of the ratio  $[G_{NC}(Q^2)]_{WY}^{\text{Higgsless}} / [G_{NC}(Q^2)]_{WY}^{\text{SM}}$  from one. This is consistent with the fact that the model parameters were chosen to make  $\alpha S$  vanish. Small deviations from one were found in the corresponding ratios for  $[G_{NC}(Q^2)]_{YY,WW}$ .

Figure 4 depicts the behavior of  $[G_{NC}(Q^2)]_{YY} / [G_{NC}(Q^2)]_{YY}^{\text{SM}}$  as calculated using eqn. (5.1). Set 1, shown by the lowest curve in the figure, is indistinguishable from the standard model. The middle curve shows the ratio for the moose with Set 2 parameters; the upper curve shows the effect of using Set 3 parameters instead. For Sets 2 and 3, the deviation from the standard model value is quite small; the visible deviation near  $\sqrt{-Q^2} \simeq 90$  GeV comes from the difference between  $c_Z M_Z$  and  $M_W$ .

The form of the correlation function  $[G_{NC}(Q^2)]_{WW}$  is derived by starting from eqn (3.6) and working in parallel with the arguments in section 6 and Ref. [7] to find

$$[G_{NC}(Q^2)]_{0,i} = \frac{e^2 M_Z^2}{Q^2(Q^2 + M_Z^2)} \left[ \prod_{z=1,2} \frac{m_z^2}{Q^2 + m_z^2} \right] \frac{\det [Q^2 + M_{(i,3]}^2]}{\det [M_{(i,3]}^2]}, \quad (8.12)$$

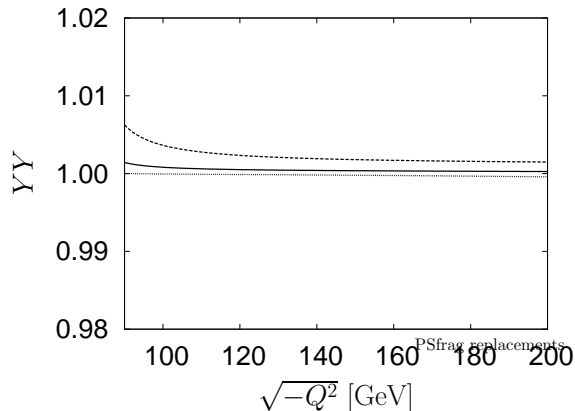


**Figure 4:**  $[G_{\text{NC}}(Q^2)]_{YY}/[G_{\text{NC}}(Q^2)]_{YY}^{\text{SM}}$  for the LEP energy range. From lowest to highest, the curves are for the Set 1, 2, and 3. parameters. Set 1 is indistinguishable from the standard model in this plot.

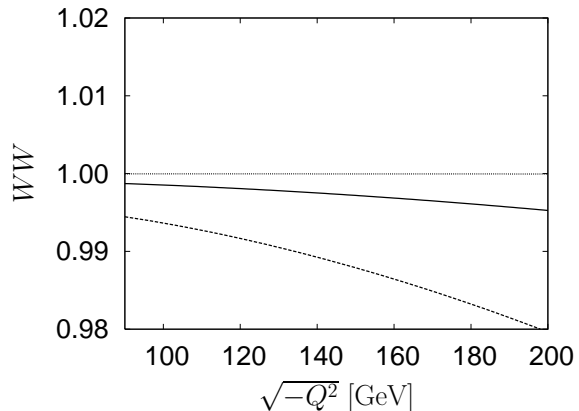


**Figure 5:**  $[G_{\text{NC}}(Q^2)]_{WW}/[G_{\text{NC}}(Q^2)]_{WW}^{\text{SM}}$  for the LEP energy range. From highest to lowest, the curves are for the Set 1, 2, and 3 parameters. Set 1 is indistinguishable from the standard model in this plot.

$$[G_{\text{NC}}(Q^2)]_{1,1} = \left[ 1 + \frac{Q^2}{\tilde{m}^2} \right] [G_{\text{NC}}(Q^2)]_{0,1} \quad (8.13)$$

We calculate the eigenvalues of matrix  $M_{(0,3)}^2$  in the four-site model to be

$$\text{Set 1 : } \quad 43.4066 \text{ GeV}, \quad 890.794 \text{ GeV}, \quad 1943.92 \text{ GeV} \quad (8.14)$$

$$\text{Set 2 : } \quad 43.4996 \text{ GeV}, \quad 972.319 \text{ GeV}, \quad 2140.13 \text{ GeV} \quad (8.15)$$

$$\text{Set 3 : } \quad 43.6216 \text{ GeV}, \quad 982.737 \text{ GeV}, \quad 4114.49 \text{ GeV} , \quad (8.16)$$

and those of matrix  $M_{(1,3)}^2$  are found to be

$$\text{Set 1 : } \quad 74.7636 \text{ GeV}, \quad 1675.68 \text{ GeV} \quad (8.17)$$

$$\text{Set 2 : } \quad 44.8651 \text{ GeV}, \quad 1008.779 \text{ GeV} \quad (8.18)$$

$$\text{Set 3 : } \quad 43.9536 \text{ GeV}, \quad 987.883 \text{ GeV}. \quad (8.19)$$

The  $[G_{\text{NC}}(Q^2)]_{WW}$  results for Sets 1, 2, and 3 are depicted in the upper, middle, and lower curves of Figure 5. Set 1 is, again, indistinguishable from the standard model. For the Set 2 parameters, the deviation of the correlation function from its standard model form is less than 0.5% even at  $\sqrt{-Q^2} = 200$  GeV; this choice of parameters seems to be phenomenologically acceptable. For Set 3, the deviation is about 2% at  $\sqrt{-Q^2} = 200$  GeV, which is too large to be phenomenologically acceptable.

## 8.2 Electroweak corrections

By construction, we expect that the electroweak corrections other than  $\alpha\delta$  will be suppressed for any of our sample sets of parameters. Because the model is Type-I [7],  $\Delta\rho = 0$ ; because

$g_{N+1}$  is small (3.22),  $\alpha T \approx 0$ ; the value of  $x_1$  was explicitly chosen (4.12) to make  $\alpha S \approx 0$ . This turns out to be the case; numerical evaluation shows  $|\alpha S| \lesssim 10^{-5}$ ,  $|\alpha T| \lesssim 10^{-5}$ ,  $|\alpha U| \lesssim 10^{-5}$ .

However, the value of  $\alpha\delta$  is not automatically small enough to agree with constraints set by data. Set 1 has the smallest value of  $x_1$ , and the corresponding value of  $\alpha\delta$  is zero to within the limits of numerical accuracy. For Set 2, the experimental upper bound [12] of order .001 is satisfied by the quantity

$$\frac{\alpha\delta}{4s_Z^2 c_Z^2} = 1 - \frac{[\xi_W]_{WW}}{4\sqrt{2}G_F M_W^2} = 0.70 \times 10^{-3}, \quad (8.20)$$

Note that the approximate value for  $\alpha\delta$  from equation (6.21) is consistent with the exact result above: the difference is precisely the size of the terms neglected in the approximation. For set 3, on the other hand,  $\alpha\delta$  lies above the experimental bound

$$\frac{\alpha\delta}{4s_Z^2 c_Z^2} = 3.04 \times 10^{-3}. \quad (8.21)$$

In other words, choosing the amount of delocalization to guarantee that the oblique correction  $\alpha S$  is small does not guarantee that the universal non-oblique correction  $\alpha\delta$  will be of acceptable size. The first requires  $x_1$  to be a function of the couplings and  $f$ -constants; the second places an absolute upper bound on the value of  $x_1$ . In our 4-site model, the most significant effect of the larger value of  $f_1$  for set 3 was to drive  $x_1$  larger – which pushed  $\alpha\delta$  too high.

## 9. Conclusions

In this note we have calculated the form of electroweak corrections in deconstructed Higgsless models for the case of a fermion whose weak properties arise from two adjacent  $SU(2)$  groups on the deconstructed lattice. We have shown that, as recently proposed in the continuum [31, 32], it is possible for the value of the electroweak parameter  $\alpha S$  to be small in such a model. Working in the deconstructed limit we have also directly evaluated the size of  $\alpha\delta$ , arising off- $Z$ -pole from the exchange of Kaluza-Klein modes [9]. This has not previously been evaluated in the continuum. In one-site delocalized Higgsless models with small values of  $\alpha S$ , we showed that the amount of delocalization is bounded to be less than of order 25% at 95%CL due to the simultaneous need to ensure unitarization of  $W_L W_L$  scattering and to provide a value of  $\alpha\delta$  that agrees with experiment. We have discussed the relation of these calculations to our previous calculations in deconstructed Higgsless models [7], and to models of extended technicolor. Finally, we presented numerical results for a four-site model, illustrating our analytic calculations. In a subsequent publication, [33], we will generalize our discussion to multi-site delocalization and discuss the effects of fermion delocalization in the continuum.

## Acknowledgments

R.S.C. and E.H.S. are supported in part by the US National Science Foundation under award PHY-0354226. M.K. acknowledges support by the 21st Century COE Program of Nagoya University provided by JSPS (15COEG01). M.T.'s work is supported in part by the JSPS Grant-in-Aid for Scientific Research No.16540226. H.J.H. is supported by the US Department of Energy grant DE-FG03-93ER40757.

## References

- [1] C. Csaki, C. Grojean, H. Murayama, L. Pilo, and J. Terning, *Gauge theories on an interval: Unitarity without a higgs*, *Phys. Rev.* **D69** (2004) 055006, [hep-ph/0305237](#).
- [2] R. Sekhar Chivukula, D. A. Dicus, and H.-J. He, *Unitarity of compactified five dimensional yang-mills theory*, *Phys. Lett.* **B525** (2002) 175–182, [[hep-ph/0111016](#)].
- [3] R. S. Chivukula and H.-J. He, *Unitarity of deconstructed five-dimensional yang-mills theory*, *Phys. Lett.* **B532** (2002) 121–128, [[hep-ph/0201164](#)].
- [4] R. S. Chivukula, D. A. Dicus, H.-J. He, and S. Nandi, *Unitarity of the higher dimensional standard model*, *Phys. Lett.* **B562** (2003) 109–117, [[hep-ph/0302263](#)].
- [5] H. J. He, “Higgsless deconstruction without boundary condition,” [arXiv:hep-ph/0412113](#).
- [6] P. W. Higgs, *Broken symmetries, massless particles and gauge fields*, *Phys. Lett.* **12** (1964) 132–133.
- [7] R. Sekhar Chivukula, E. H. Simmons, H.-J. He, M. Kurachi, and M. Tanabashi, *Electroweak corrections and unitarity in linear moose models*, *Phys. Rev.* **D71** (2005) 035007, [hep-ph/0410154](#).
- [8] R. S. Chivukula, E. H. Simmons, H.-J. He, M. Kurachi, and M. Tanabashi, *The structure of corrections to electroweak interactions in higgsless models*, *Phys. Rev.* **D70** (2004) 075008, [hep-ph/0406077](#).
- [9] R. S. Chivukula, E. H. Simmons, H.-J. He, M. Kurachi, and M. Tanabashi, *Universal non-oblique corrections in higgsless models and beyond*, *Phys. Lett.* **B603** (2004) 210–218, [[hep-ph/0408262](#)].
- [10] N. Arkani-Hamed, A. G. Cohen, and H. Georgi, *(de)constructing dimensions*, *Phys. Rev. Lett.* **86** (2001) 4757–4761, [[hep-th/0104005](#)].
- [11] C. T. Hill, S. Pokorski, and J. Wang, *Gauge invariant effective lagrangian for kaluza-klein modes*, *Phys. Rev.* **D64** (2001) 105005, [[hep-th/0104035](#)].
- [12] R. Barbieri, A. Pomarol, R. Rattazzi, and A. Strumia, *Electroweak symmetry breaking after lep1 and lep2*, *Nucl. Phys.* **B703** (2004) 127, [hep-ph/0405040](#).
- [13] R. S. Chivukula, H.-J. He, J. Howard, and E. H. Simmons, *The structure of electroweak corrections due to extended gauge symmetries*, *Phys. Rev.* **D69** (2004) 015009, [[hep-ph/0307209](#)].

- [14] R. Casalbuoni, S. De Curtis, D. Dominici, and R. Gatto, *Effective weak interaction theory with possible new vector resonance from a strong higgs sector*, *Phys. Lett.* **B155** (1985) 95.
- [15] R. Casalbuoni *et. al.*, *Degenerate bess model: The possibility of a low energy strong electroweak sector*, *Phys. Rev.* **D53** (1996) 5201–5221, [[hep-ph/9510431](#)].
- [16] R. Casalbuoni, S. De Curtis, and D. Dominici, *Moose models with vanishing  $s$  parameter*, *Phys. Rev.* **D70** (2004) 055010, [[hep-ph/0405188](#)].
- [17] M. Bando, T. Kugo, S. Uehara, K. Yamawaki, and T. Yanagida, *Is rho meson a dynamical gauge boson of hidden local symmetry?*, *Phys. Rev. Lett.* **54** (1985) 1215.
- [18] M. Bando, T. Kugo, and K. Yamawaki, *On the vector mesons as dynamical gauge bosons of hidden local symmetries*, *Nucl. Phys.* **B259** (1985) 493.
- [19] M. Bando, T. Fujiwara, and K. Yamawaki, *Generalized hidden local symmetry and the  $a_1$  meson*, *Prog. Theor. Phys.* **79** (1988) 1140.
- [20] M. Bando, T. Kugo, and K. Yamawaki, *Nonlinear realization and hidden local symmetries*, *Phys. Rept.* **164** (1988) 217–314.
- [21] M. Harada and K. Yamawaki, *Hidden local symmetry at loop: A new perspective of composite gauge boson and chiral phase transition*, *Phys. Rept.* **381** (2003) 1–233, [[hep-ph/0302103](#)].
- [22] C. Csaki, C. Grojean, L. Pilo, and J. Terning, *Towards a realistic model of higgsless electroweak symmetry breaking*, *Phys. Rev. Lett.* **92** (2004) 101802, [[hep-ph/0308038](#)].
- [23] Y. Nomura, *Higgsless theory of electroweak symmetry breaking from warped space*, *JHEP* **11** (2003) 050, [[hep-ph/0309189](#)].
- [24] R. Barbieri, A. Pomarol, and R. Rattazzi, *Weakly coupled higgsless theories and precision electroweak tests*, *Phys. Lett.* **B591** (2004) 141, [[hep-ph/0310285](#)].
- [25] H. Davoudiasl, J. L. Hewett, B. Lillie, and T. G. Rizzo, *Higgsless electroweak symmetry breaking in warped backgrounds: Constraints and signatures*, *Phys. Rev.* **D70** (2004) 015006, [[hep-ph/0312193](#)].
- [26] R. Foadi, S. Gopalakrishna, and C. Schmidt, *Higgsless electroweak symmetry breaking from theory space*, *JHEP* **03** (2004) 042, [[hep-ph/0312324](#)].
- [27] G. Burdman and Y. Nomura, *Holographic theories of electroweak symmetry breaking without a higgs boson*, *Phys. Rev.* **D69** (2004) 115013, [[hep-ph/0312247](#)].
- [28] H. Davoudiasl, J. L. Hewett, B. Lillie, and T. G. Rizzo, *Warped higgsless models with ir-brane kinetic terms*, *JHEP* **05** (2004) 015, [[hep-ph/0403300](#)].
- [29] J. L. Hewett, B. Lillie, and T. G. Rizzo, *Monte carlo exploration of warped higgsless models*, *JHEP* **10** (2004) 014, [[hep-ph/0407059](#)].
- [30] M. Perelstein, *Gauge-assisted technicolor?*, *JHEP* **10** (2004) 010, [[hep-ph/0408072](#)].
- [31] G. Cacciapaglia, C. Csaki, C. Grojean, and J. Terning, *Curing the ills of higgsless models: The  $s$  parameter and unitarity*, [[hep-ph/0409126](#)].
- [32] R. Foadi, S. Gopalakrishna, and C. Schmidt, *Effects of fermion localization in higgsless theories and electroweak constraints*, *Phys. Lett.* **B606** (2005) 157, [[hep-ph/0409266](#)].

- [33] R. Sekhar Chivukula, E. H. Simmons, H.-J. He, M. Kurachi, and M. Tanabashi, to be published.
- [34] H. Georgi, *A tool kit for builders of composite models*, *Nucl. Phys.* **B266** (1986) 274.
- [35] M. E. Peskin and T. Takeuchi, *Estimation of oblique electroweak corrections*, *Phys. Rev.* **D46** (1992) 381–409.
- [36] G. Altarelli and R. Barbieri, *Vacuum polarization effects of new physics on electroweak processes*, *Phys. Lett.* **B253** (1991) 161–167.
- [37] G. Altarelli, R. Barbieri, and S. Jadach, *Toward a model independent analysis of electroweak data*, *Nucl. Phys.* **B369** (1992) 3–32.
- [38] L. J. Hall and S. F. King, *Probing compositeness on the  $z$  pole*, *Nucl. Phys.* **B287** (1987) 551.
- [39] R. S. Chivukula and H. Georgi, *Phenomenology of composite technicolor standard models*, *Phys. Rev.* **D36** (1987) 2102.
- [40] L. Randall and R. S. Chivukula, *Could composite interactions be detected at  $s^{**}(1/2) = m(z)$ ?*, *Nucl. Phys.* **B326** (1989) 1.
- [41] R. S. Chivukula, S. B. Selipsky, and E. H. Simmons, *Nonoblique effects in the  $z$   $b$  anti- $b$  vertex from etc dynamics*, *Phys. Rev. Lett.* **69** (1992) 575–577, [[hep-ph/9204214](#)].
- [42] M. Golden and L. Randall, *Radiative Corrections To Electroweak Parameters In Technicolor Theories*, *Nucl. Phys.* **B361** (1991) 3.
- [43] B. Holdom and J. Terning, *Large Corrections To Electroweak Parameters In Technicolor Theories*, *Phys. Lett.* **B247** (1990) 88.
- [44] S. Eidelman *et al.* [Particle Data Group], *Review of Particle Physics*, *Phys. Lett.* **B592** (2004) 1.